Long noncoding RNA-mediated intrachromosomal interactions promote imprinting at the *Kcnq1* locus

He Zhang,[1,2,3,4] Michael J. Zeitz,[4] Hong Wang,[1,4] Beibei Niu,[2,3] Shengfang Ge,[2,3] Wei Li,[1] Jiuwei Cui,[1] Guanjun Wang,[1] Guanxiang Qian,[2,3] Michael J. Higgins,[5] Xianqun Fan,[2,3] Andrew R. Hoffman,[4] and Ji-Fan Hu[1,4]

[1]Stem Cell and Cancer Center, First Affiliated Hospital, Jilin University, Changchun 130061, People's Republic of China
[2]Department of Ophthalmology and [3]Department of Biochemistry and Molecular Biology, Ninth People's Hospital, Shanghai JiaoTong University School of Medicine, Shanghai 200011, People's Republic of China
[4]Veterans Affairs Palo Alto Health Care System, Stanford University Medical School, Palo Alto, CA 94304
[5]Department of Molecular and Cellular Biology, Roswell Park Cancer Institute, Buffalo, NY 14263

Kcnq1ot1 is a long noncoding ribonucleic acid (RNA; lncRNA) that participates in the regulation of genes within the *Kcnq1* imprinting domain. Using a novel RNA-guided chromatin conformation capture method, we demonstrate that the 5′ region of *Kcnq1ot1* RNA orchestrates a long-range intrachromosomal loop between KvDMR1 and the *Kcnq1* promoter that is required for maintenance of imprinting. PRC2 (polycomb repressive complex 2), which participates in the allelic repression of *Kcnq1*, is also recruited by *Kcnq1ot1* RNA via EZH2. Targeted suppression of *Kcnq1ot1* lncRNA prevents the creation of this long-range intrachromosomal loop and causes loss of *Kcnq1* imprinting. These observations delineate a novel mechanism by which an lncRNA directly builds an intrachromosomal interaction complex to establish allele-specific transcriptional gene silencing over a large chromosomal domain.

Introduction

Although most of the mammalian genome is transcribed into RNA, the majority of this RNA does not code for proteins (Prasanth and Spector, 2007). Long noncoding RNAs (lncRNAs) represent a very large subgroup of the mammalian transcriptome. Unlike most mRNAs, lncRNAs are usually intronless and are often transcribed in the antisense orientation with respect to associated protein-coding genes (Lee, 2012). A recent study has demonstrated that some lncRNAs are involved in the epigenetic regulation in cis and in trans of a cluster of genes within large chromosomal domains by forming scaffolds to recruit and interact with the chromatin-modifying machinery (Nagano and Fraser, 2011).

Kcnq1ot1, which is transcribed into a 91-kb noncoding RNA, is imprinted and expressed exclusively from the paternal chromosome in an antisense direction with respect to *Kcnq1* (Smilinich et al., 1999; Pandey et al., 2008; Redrup et al., 2009). A more detailed mapping of transcription products suggests that in stem cells, the *Kcnq1ot1* may be transcribed as a 471-kb lncRNA (Golding et al., 2011). In the mouse, *Kcnq1ot1* maps to the *Kcnq1* domain located at the distal end of chromosome 7. Its human orthologue is located on human chromosome 11, and epimutations of this region have been implicated in the Beckwith–Wiedemann syndrome, a disorder of prenatal overgrowth, and a predisposition to embryonal malignancies, such as Wilms' tumor (Lee et al., 1999). In close to 50% of individuals with Beckwith–Wiedemann syndrome, loss of maternal-specific methylation at KvDMR1, the putative imprinting control region (ICR) within intron 10 of the *KCNQ1* gene, leads to expression of the normally silent maternal allele of the *KCNQ1OT1* transcript (Lee et al., 1999; Smilinich et al., 1999; Fitzpatrick et al., 2002).

Kcnq1ot1 RNA is a bidirectional silencer that regulates genes in cis over ∼1 Mb in the *Kcnq1* imprinting domain, which contains 8–10 maternally expressed protein coding genes (Mancini-DiNardo et al., 2003; Thakur et al., 2004). The *Kcnq1ot1* promoter is located in a differentially methylated ICR (*Kcnq1* ICR, called KvDMR1) in intron 10 of the *Kcnq1* gene, and its

Correspondence to Ji-Fan Hu: jifan@stanford.edu; or Andrew R. Hoffman: arhoffman@stanford.edu.

A.R. Hoffman and J.-F. Hu contributed equally to this paper.

Abbreviations used in this paper: 3C, chromosome conformation capture; BAC, bacterial artificial chromosome; ChIP, chromatin immunoprecipitation; ChOP, chromatin oligonucleotide-affinity precipitation; dCTP, deoxy-CTP; DID, DNA interaction domain; ICR, imprinting control region; lncRNA, long noncoding RNA; MEF, mouse embryonic fibroblast; R3C, RNA-guided 3C; RT, reverse transcription; SNP, single nucleotide polymorphism; ZF, zinc finger.

The Rockefeller University Press $30.00
J. Cell Biol. Vol. 204 No. 1 61–75
www.jcb.org/cgi/doi/10.1083/jcb.201304152

transcriptional activity is controlled by DNA methylation and a variety of histone modifications. Because its promoter on the maternal chromosome is methylated, *Kcnq1ot1* is expressed only from the paternal chromosome.

Although *Kcnq1ot1* RNA regulates allelic expression of both ubiquitously and placenta-specific imprinted genes (Kanduri, 2011), the mechanisms for allelic silencing of these two classes of genes over long distances remain enigmatic. KvDMR1, the region that carries the imprinting signal to control imprinting, is ∼200 kb away from the *Kcnq1* promoter, one of its target genes, and it is not known how this imprinting control message is delivered over this long distance. Several investigators have shown that *Kcnq1ot1* interacts with chromatin, and it is possible that this relationship underlies the ability of the lncRNA to control the imprinting of genes in this region (Murakami et al., 2007; Terranova et al., 2008). In this communication, we report the use of a novel RNA-guided chromosome conformation capture (3C; R3C) approach to delineate the role of *Kcnq1ot1* in long-range chromatin interactions. Using standard 3C (Dekker et al., 2002), we found that *Kcnq1ot1* lncRNA functions as a necessary scaffold molecule to orchestrate a long-range intrachromosomal loop between KvDMR1 and the *Kcnq1* promoter, recruiting a variety of proteins, including PRC2 (polycomb repressive complex 2), to maintain monoallelic expression of the cluster of genes in the *Kcnq1* imprinting domain.

Results

A novel R3C approach to detect the RNA–DNA interaction

To explore the mechanism by which *Kcnq1ot1* lncRNA regulates the imprinting of genes in cis over several hundred kilobases of DNA, we devised a novel method called R3C to detect RNA–DNA interactions (Fig. 1 A). In this approach, the DNA-binding RNA is first reverse transcribed into double-stranded cDNA with biotin labeling. After digestion with restriction enzyme EcoRI, the lncRNA-converted double-strand cDNA is ligated to adjacent genomic DNAs by T4 DNA ligase. The biotinylated *Kcnq1ot1* cDNA–DNA complex is then separated from other DNA–DNA products by streptavidin pull-down using paramagnetic Dynabeads and analyzed by PCR using RNA–DNA interaction-specific primers.

To demonstrate the feasibility of the method, we set up controls to validate each critical step of the R3C assay. First, we determined whether the restriction enzyme EcoRI was active on biotin-labeled double-strand cDNAs, as the enzyme activity can be inhibited by overlapping methylated CpGs. We used PCR to amplify three known DNA fragments with overlapping CpGs at the EcoRI site (cGAATTCg, or GAATTCg; capital letters are the EcoRI site, and the lowercase letters are the EcoRI-overlapping CGs that can be methylated in the genome; Fig. S1 A) with 1:10 biotin–deoxy-CTP (dCTP)/dCTP added in the PCR reaction. The biotinylated PCR DNAs were then used as substrates to determine the enzymatic activity of EcoRI. We found that the DNA fragments that were labeled with 10% biotin-dCTP did not interfere with the activity of EcoRI (Fig. S1 A, lanes 2, 4, and 6).

Next, we tested whether *Kcnq1ot1* lncRNA could be reverse transcribed and amplified by PCR after it was cross-linked with chromatin. The *Kcnq1ot1*-associated chromatin fragments were fixed by formaldehyde and digested by EcoRI to shear the genomic DNA. The cross-linked *Kcnq1ot1* fragments were pulled down using histone H3 antibody–protein G magnetic beads to allow the subsequent reactions, such as reverse transcription (RT) and ligation, to take place on solid substrate-associated chromatins. After the treatment with DNase I to digest the DNA, the *Kcnq1ot1* lncRNA was reverse transcribed in the presence of either *Kcnq1ot1*-specific or *Kcnq1*-specific RT primers (Fig. S1 B). We detected *Kcnq1ot1* cDNA products but not *Kcnq1* cDNA products, demonstrating the availability of chromatin cross-linked RNA for the RT-PCR reaction.

Finally, we determined whether the second-strand cDNA could be synthesized from the chromatin-linked *Kcnq1ot1* lncRNA without losing its cross-link to the chromatin DNA after digestion with the RNase H in the reaction. The chromatin-bound lncRNA was pulled down using anti–histone H3 antibody–protein G magnetic beads and was reverse transcribed by ThermoScript transcriptase using a *Kcnq1ot1*-specific primer, #R4A (Fig. S1 C). After washing away the remaining primer and RT enzyme, the second-strand cDNA was synthesized on protein G magnetic beads in the presence of 1:10 biotin-dCTP/dCTP. The biotinylated double-strand cDNAs were released from the protein G beads and were separated from genomic DNAs by streptavidin beads for PCR detection. We detected PCR products for the *Kcnq1ot1* second-strand cDNA from the chromatin beads using the #R4A downstream PCR primers (H147/H148; Fig. S1 C, lane 1), indicating the presence of an intact double-strand cDNA–chromatin complex. No PCR products were detected using the #R4A upstream primers (H145/H263; Fig. S1 C, lane 6), excluding the possibility of contamination of the biotin nick-labeled genomic DNA during the replacement reaction of the second-strand cDNA synthesis. These experiments demonstrate that the R3C enzyme digestion and ligation can occur on the chromatin DNA–lncRNA–cDNA complex.

Capturing *Kcnq1ot1* lncRNA–genomic DNA interactions by R3C

We then used the R3C approach to detect the ligated *Kcnq1ot1* lncRNA–DNA product using a PCR primer set consisting of one primer from the *Kcnq1ot1* cDNA and the other primer from the DNA region with which it interacts and mapped the RNA–DNA interaction using primer sets covering the entire *Kcnq1ot1* lncRNA (Fig. 1 B). We detected the direct interaction of *Kcnq1ot1* noncoding RNA (Ra and Rb sites) with both the *Kcnq1* promoter (D1 and D2 sites; Fig. 1 B, left, lanes 1 and 2) and the *Kcnq1* ICR (KvDMR1; D5 and D6 sites; Fig. 1 B, right, lanes 5 and 6). No interactions were detected in nonbiotin-labeled samples (Fig. 1 B, lanes 3, 4, 7, and 8). We also tested the specificity using a series of negative controls. No R3C products were observed when the sample was pretreated with RNase A to destroy *Kcnq1ot1* lncRNA or when R3C was performed in the absence of RT (Fig. S2, RT−) or at the off-target EcoRI sites located 10 kb downstream of the KvDMR1 on chromosome 7 (Fig. S2). R3C products were confirmed by sequencing

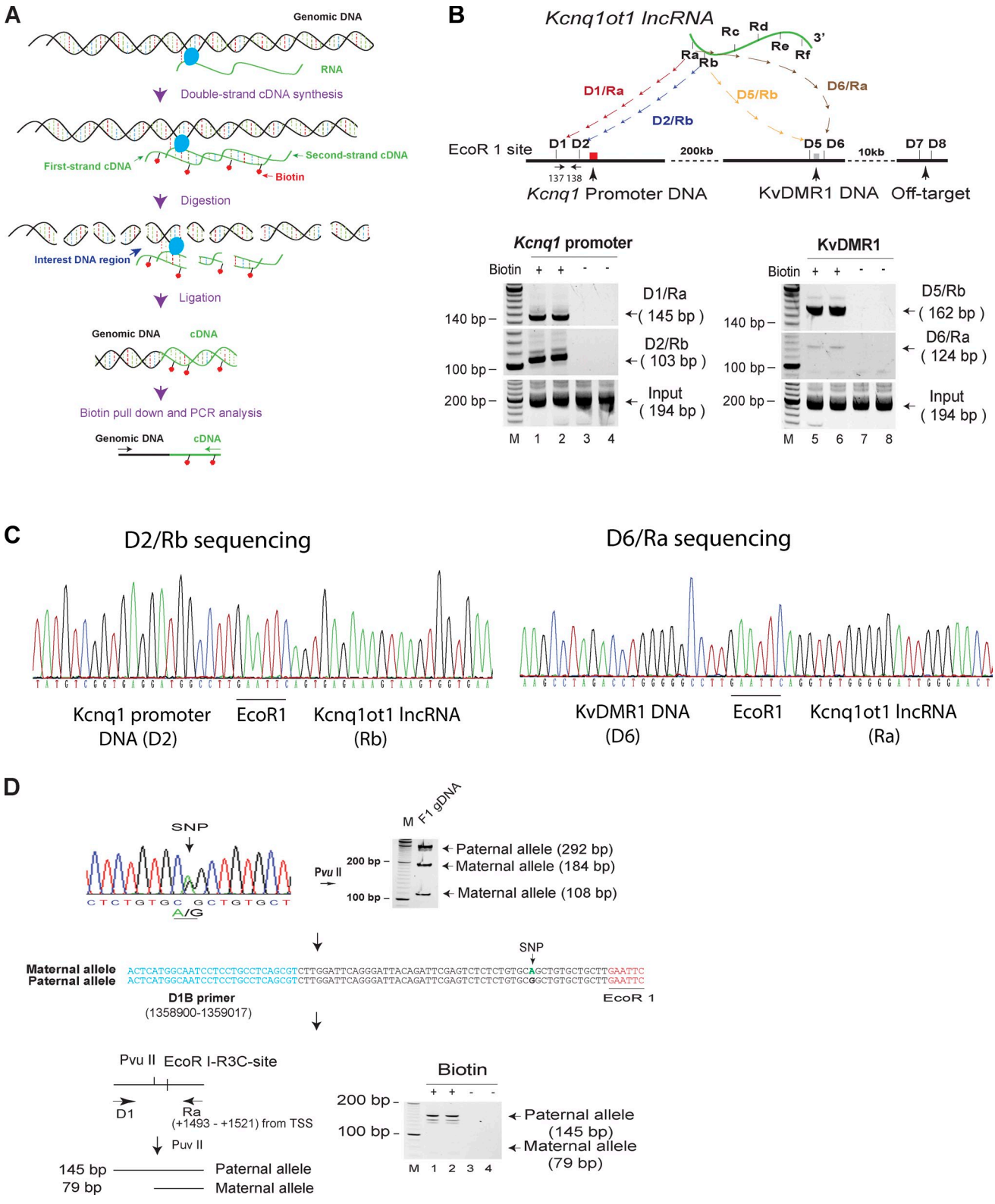

Figure 1. **A novel RNA 3C assay is developed to detect the interaction of *Kcnq1ot1* with *Kcnq1* promoter and KvDMR1.** (A) The schematic diagram shows the procedure for the R3C assay. Red dots, biotin; blue ovals, cross-linked protein; horizontal arrows above the ligated DNA show primers used to detect the R3C products. (B) R3C detects the *Kcnq1ot1* lncRNA–DNA interaction. PCR detection sites were labeled as D1–D8 for genomic DNA and Ra–Rf for *Kcnq1ot1* lncRNA. M, 100-bp marker. Note the interaction of *Kcnq1ot1* lncRNA at regions (Ra and Rb) with the *Kcnq1* promoter (D1 and D2; left) and with KvDMR1 (D5 and D6; right). (C) R3C products are confirmed by DNA sequencing. The R3C products derived from the *Kcnq1* promoter–*Kcnq1ot1* lncRNA interaction (D2/Rb) and the KvDMR1–*Kcnq1ot1* lncRNA interaction (D6/Ra) were cloned and sequenced. Note that the R3C products contain the EcoRI (5′-GAATTC-3′) that was flanked on both sides by chromatin DNA and Kcnq1ot1 cDNA. (D) The *Kcnq1ot1* RNA–chromatin interaction is allele specific. After PCR, the two parental alleles were distinguished using the PuvII restriction enzyme. Input, genomic DNA collected before biotin pull-down. D1 and Ra, PCR primers used to detect the lncRNA–DNA interaction.

and confirmed the identity of the ligated *Kcnq1* promoter/Kcnq1ot1 cDNA (Fig. 1 C, left) and the ligated *Kcnq1* promoter / KvDMR1 (Fig. 1 C, right).

To determine whether this RNA–DNA interaction is allele-specific, we used a mouse fibroblast cell line (MBW2) derived from an F1 cross between *Mus spretus* and a C57B/6 mouse. We sequenced a 292-bp genomic DNA covering the EcoRI site and found an A/G single nucleotide polymorphism (SNP) on the PvuII site that distinguishes the two parental alleles (Fig. 1 D, top). Using this SNP to separate the allelic R3C products, we found that *Kcnq1ot1* lncRNA interacted exclusively with the paternal *Kcnq1* promoter (Fig. 1 D, bottom, lanes 1 and 2).

Loss of the RNA–DNA interaction after *Kcnq1ot1* silencing

To confirm this allelic RNA–DNA interaction, we specifically silenced the paternal *Kcnq1ot1* lncRNA using a de novo DNA methylation approach (Zhang et al., 2011) based on the known regulatory mechanism of this imprinting locus. The allelic expression of *Kcnq1ot1* is regulated by allele-specific DNA methylation. The mouse *Kcnq1* ICR (KvDMR1) contains two CpG islands: CpG1 and CpG2 (Fig. 2 A; Paulsen et al., 2005). CpG1 island, located ∼200 kb downstream of the *Kcnq1* promoter, overlaps with the *Kcnq1ot1* promoter, and contains two critical CTCF binding sites (CTS1 and CTS2; Fig. 2 B). The CpG1 DNA is paternally unmethylated and maternally methylated, thereby allowing the exclusive expression of *Kcnq1ot1* from the paternal chromosome. CTCF binds to the unmethylated paternal allele and may participate in the regulation of the expression of *Kcnq1ot1* (Fitzpatrick et al., 2007).

We reasoned that paternal *Kcnq1ot1* expression would be abolished if the KvDMR1 CpG island was de novo methylated to the level seen in the maternal promoter. For this purpose, we synthesized a recombinant CTCF analogue (zinc finger [ZF]-Sss1) by replacing the functional C terminus of CTCF with CpG methylase Sss1, while maintaining the ZF DNA-binding domain that binds to CTS1 and CTS2. When this fusion protein binds to CTCF binding sites, it has the potential to methylate nearby CpG dinucleotides. With this approach, we attempted to induce de novo DNA methylation in the *Kcnq1ot1* promoter and thereby abolish the allelic gene expression of *Kcnq1ot1* without altering local chromatin structure.

The ZF-*Sss1* gene was packaged into lentiviruses and transduced into F1 mouse fibroblast cells (MBW2) that maintain normal *Kcnq1ot1* imprinting. Stable cell clones were selected using puromycin. Using sodium bisulfite sequencing, we found that the *Kcnq1ot1* promoter region was hemimethylated in control cells, i.e., unmethylated on the paternal allele (Fig. 2 B, top). In lentivirus-infected cells, however, the expressed ZF-Sss1 bound to CTCF sites in the CpG1 island of the paternal allele and induced de novo DNA methylation in the paternal *Kcnq1ot1* promoter (Fig. 2 B, middle and bottom).

We then used RT-PCR to examine whether the targeted DNA methylation would suppress the expression of *Kcnq1ot1* lncRNA. In control cells, *Kcnq1ot1* lncRNA was detected by three primer sets covering three different regions of the *Kcnq1ot1* lncRNA (Fig. 2 C, lanes 1 and 2) at sites A, E, and B. In ZF-Sss1–expressing cell clones, *Kcnq1ot1* expression was significantly reduced in association with de novo DNA methylation (Fig. 2 C, lanes 3 and 4). These data demonstrate that the recombinant protein ZF-Sss1 is able to methylate CpG dinucleotides in the paternal *Kcnq1ot1* promoter region, leading to silencing of paternal *Kcnq1ot1* gene expression. We will refer to these cells as *Kcnq1ot1* methylation "silenced" cells to distinguish them from the gene deletion knockout and shRNA depletion cells in the following text.

We then examined whether *Kcnq1ot1* silencing would affect the *Kcnq1ot1* RNA–DNA interaction. Using R3C, we show that in MBW2 control cells, *Kcnq1ot1* directly interacted with the *Kcnq1* promoter (Fig. 2 D, left, lanes 1 and 2). In *Kcnq1ot1*-silenced cells, however, no interaction was detected (Fig. 2 D, left, lanes 5 and 6). Similarly, no interaction was detected at the KvDMR1 in the *Kcnq1ot1*-silenced cells (Fig. 2 D, right, lanes 5 and 6).

We validated this finding by examining *Kcnq1ot1* knockout mouse embryonic fibroblasts (MEFs), in which the 2.8-kb KvDMR1 fragment containing the *Kcnq1ot1* promoter had been deleted (Fitzpatrick et al., 2002). In both the wild-type cells and in cells in which the deletion was maternally inherited (Fig. 2 E, −(M)/+), we detected interactions of *Kcnq1ot1* noncoding RNA with the *Kcnq1* promoter DNA (Fig. 2 E, D2/Rb) and with KvDMR1 (Fig. 2 E, left, lanes 1–3, D5/Rb). These interactions were completely abolished in those cells in which the deletion was paternally inherited (Fig. 2 E, left, lanes 7 and 8, +/−(P)).

We further confirmed this finding in a third *Kcnq1ot1* depletion model using a standard RNAi approach. Three shRNAs were used to target the 5′ region (4 kb; A-11), the middle (41 kb; D-11), and the 3′ end (71 kb; G-12) of *Kcnq1ot1* (Fig. 2 A). These shRNAs were packaged into lentiviruses and transduced into F1 mouse fibroblasts (MBW2) that maintain normal *Kcnq1ot1* imprinting. Stable cell clones were selected using puromycin, and the knockdown of *Kcnq1ot1* by shRNA was confirmed using both RT-PCR and quantitative PCR (Fig. S3, A–C). Using R3C, we show that in both the wild-type and control shRNA cells (shK1, shH19, and shNespas), *Kcnq1ot1* directly interacted with the *Kcnq1* promoter (Fig. 2 F, D2/Rb) and KvDMR1 (Fig. 2 F, D5/Rb). However, these interactions were lost in the *Kcnq1ot1* knockdown A11 and G-12 cells (Fig. 2 F, right top and middle, lanes 11 and 13). This lncRNA–DNA interaction was also confirmed by a chromatin oligonucleotide-affinity precipitation (ChOP) method (Fig. S4; Mariner et al., 2008; Pandey et al., 2008). Collectively, our data from these three distinct models demonstrate an allele-specific interaction between the *Kcnq1ot1* lncRNA and KvDMR1–*Kcnq1* promoter DNA regions.

Kcnq1ot1 lncRNA orchestrates a long-range intrachromosomal loop between the *Kcnq1* promoter and the KvDMR1

Because *Kcnq1ot1* lncRNA interacts with both the *Kcnq1* promoter and the KvDMR1, which are 200 kb apart, we hypothesized that the *Kcnq1ot1* lncRNA scaffolds these long-distance DNA regions to form an intrachromosomal structure, which is critical for the maintenance of allelic expression of genes in this

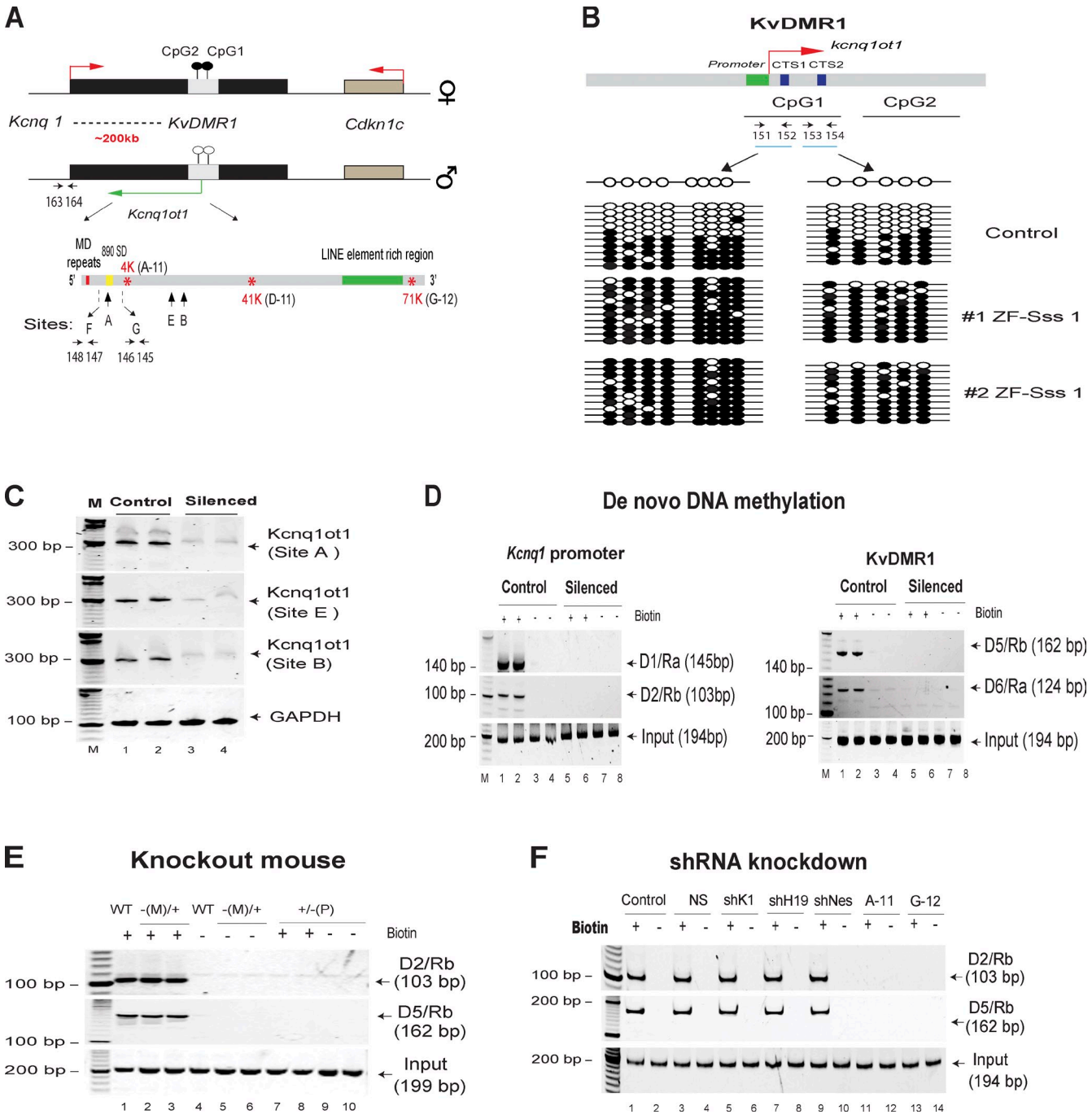

Figure 2. **The lncRNA–chromatin interaction is lost after targeted DNA methylation-mediated knockdown of *Kcnq1ot1*.** (A) The diagram shows the allelic expression of genes in the *Kcnq1* imprinting domain on mouse chromosome 7. Red/green arrows, direction of allelic expression; vertical arrows (A, E, B, F, and G), PCR detection of *Kcnq1ot1* lncRNA; stars, location of shRNA targeting sites (A-11, D-11, and G-12); ovals, CpG islands (black, methylated; white, unmethylated). 890 SD, 890-kb silencing domain. (B) Bisulfite DNA sequencing confirmed the induced DNA methylation in the *Kcnq1ot1* promoter. After sodium bisulfite treatment, genomic DNA was amplified by PCR primers (#151/152 and #153/154), cloned in the TA vector (Invitrogen), and sequenced. A total of 13 CpG dinucleotides at the KvDMR1 was examined. Each line represents a single sequenced PCR molecule. Black circles represent methylated CpG dinucleotides, and white circles represent unmethylated CpG dinucleotides. Control, wild-type cells; second and third rows, *Kcnq1ot1*-silenced cells. CTS1 and 2, CTCF binding sites 1 and 2. (C) Targeted DNA methylation silences the *Kcnq1ot1* lncRNA in F1 mouse fibroblast cells. *GAPDH* was used as a control. Sites A, E, and B are nucleotides 999–1,299, 22,445–22,745, and 31,019–31,315 from the *Kcnq1ot1* transcription start site, respectively. (D) *Kcnq1ot1* lncRNA silencing by targeted DNA methylation induces loss of the lncRNA–DNA interaction. The *Kcnq1ot* lncRNA–chromatin interactions were detected at the D1/Ra and D2/Rb sites for the *Kcnq1* promoter and the D6/Ra and D5/Rb sites for KvDMR1 as shown in Fig. 1 B. (E) The lncRNA–DNA interaction is abolished in *Kcnq1ot1* knockout MEFs. WT, wild type; −(M)/+, maternally inherited mutants; +/−(P), paternally inherited mutants. (F) *Kcnq1ot1* lncRNA depletion by shRNA abrogates the lncRNA–DNA interaction. The *Kcnq1ot* lncRNA–chromatin interactions were detected at the 2/b site for the *Kcnq1* promoter and the 5/b site for KvDMR1. NS, nonsilencing control. A-11 and G-12, shRNA. M, 100-bp marker.

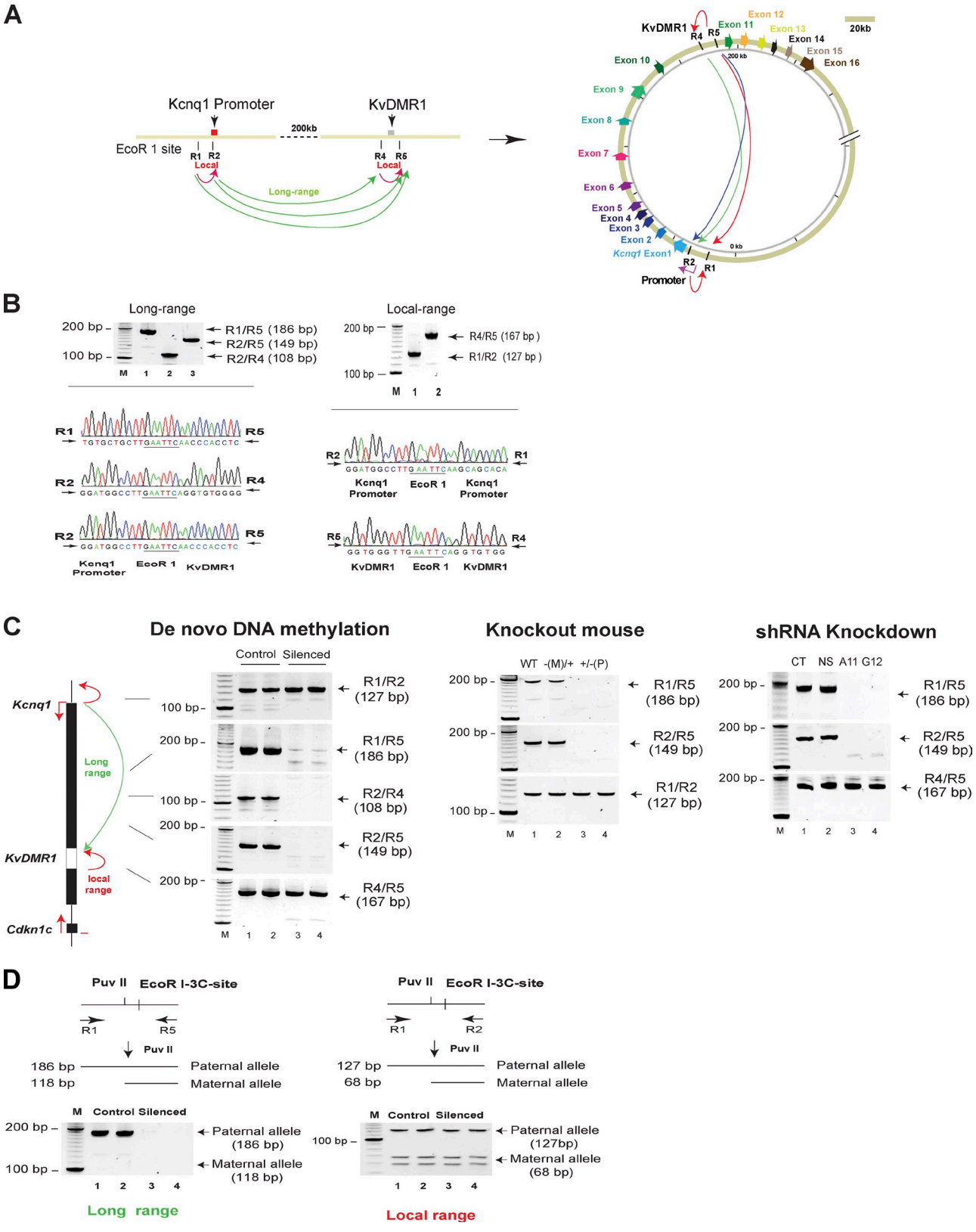

Figure 3. **The *Kcnq1* promoter and KvDMR1 interact through intrachromosomal looping.** (A) Schematic diagram shows the EcoRI sites in the *Kcnq1* imprinting locus for the 3C assay. R1–R5, EcoRI sites. (B) The 3C assay detects the long-range and local chromatin interactions. (C) Long-range intrachromosomal interactions between the *Kcnq1* promoter and KvDMR1 are abrogated in *Kcnq1ot1* DNA methylation-silenced cells, knockout mutant mouse, and shRNA-depletion cells. Silenced, *Kcnq1ot1*-suppressed cells by targeted DNA methylation; control, wild-type cells. Knockout: WT, wild-type cells; −(M)/+, maternally inherited mutant; +/−(P), paternally inherited mutant. shRNA depletion: CT, control; NS, nonsilencing shRNA control; A11 and G12, *Kcnq1ot1* shRNAs. (D) The chromatin interactions at the *Kcnq1* locus are allele specific. After PCR, the parental alleles were distinguished by PuvII polymorphic restriction enzyme. M, 100-bp marker.

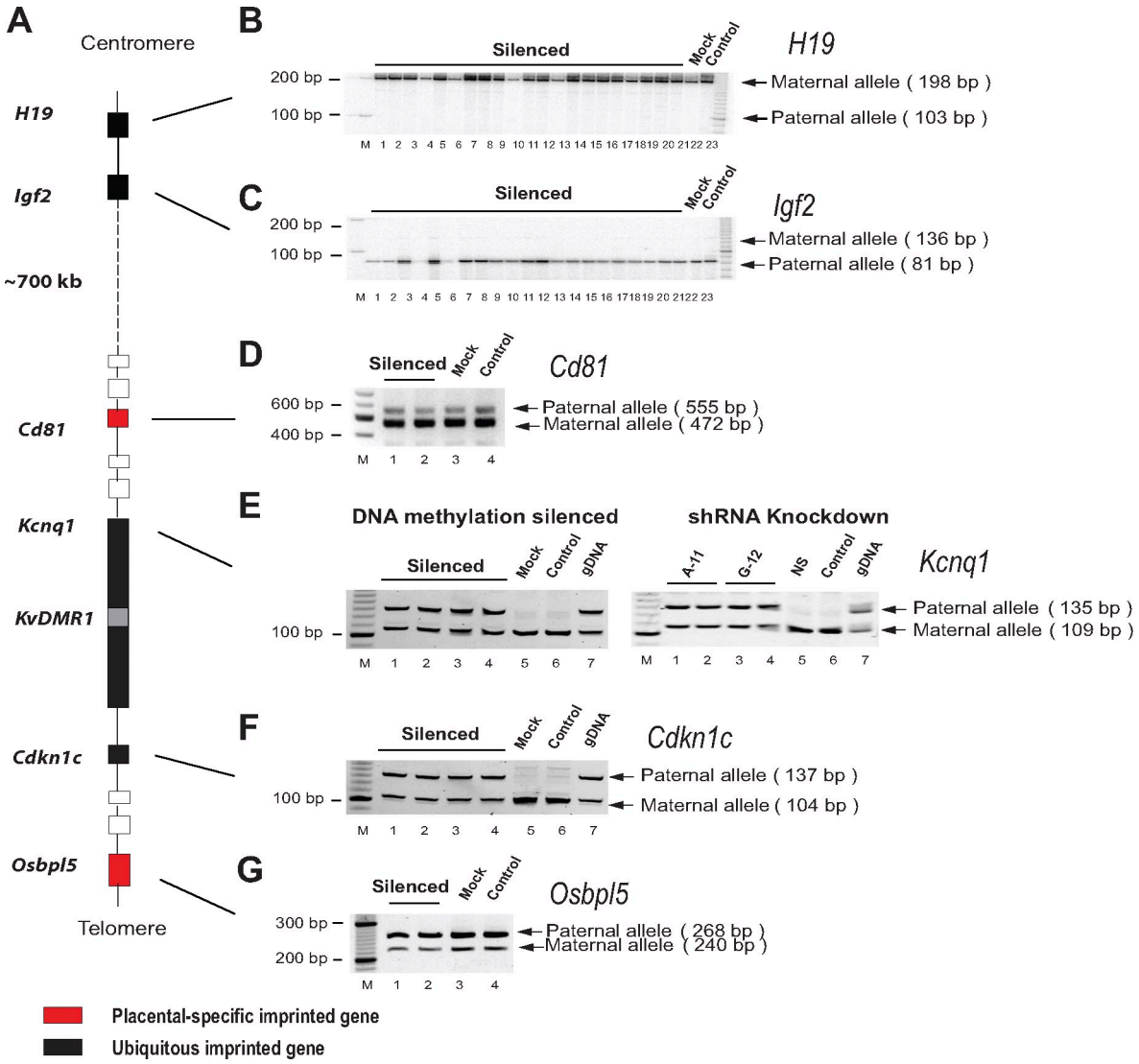

Figure 4. **Genomic imprinting of *Kcnq1* and *Cdkn1c* is abolished in *Kcnq1ot1*-silenced cells.** (A) Physical map of the *Kcnq1* locus shows the placental-specific and ubiquitously imprinted genes. (B–G) The imprinting status of *H19*, *Igf2*, *Cd81*, *Kcnq1*, *Cdkn1c*, and *Osbp15* was determined by polymorphic restriction enzymes FoxI (B), DpnII (C), RsaI (D), EcoRV (E), AvaI (F), and BfaI (G), respectively. gDNA, genomic DNA used as the positive control; mock, empty lentiviral vector; control, untreated cells; NS, nonsilencing shRNA control; A-11 and G-12, *Kcnq1ot1* shRNAs. Lanes 1–21 in B and C represent the different puromycin-selected ZF-Sss1 colony RNAs transcribed for the analysis of *Igf2* (B) and *H19* imprinting (C). M, 100-bp marker.

imprinted region. We therefore used 3C (Dekker, 2006; Li et al., 2008) to assess the potential chromatin interactions between these two DNA regions.

Cells were fixed with 2% formaldehyde, digested with restriction enzyme EcoRI, and then ligated with T4 DNA ligase to examine the remote interaction between the *Kcnq1* promoter and KvDMR1 that are 200 kb apart (Fig. 3 A). In control mouse fibroblasts that maintain normal *Kcnq1ot1* expression, we found that the KvDMR1 region (R4 and R5) directly interacted with the *Kcnq1* promoter (R1 and R2; Fig. 3 B, top left, lanes 1–3), suggesting the presence of a long-range intrachromosomal loop. Local chromosomal interactions within KvDMR1 and within the *Kcnq1* promoter regions were also detected (Fig. 3 B, top right, lanes 1 and 2, R4/R5 and R1/R2). These intrachromosomal interaction PCR products were confirmed by TA cloning and sequencing (Fig. 3 B, bottom). However, the long-range intrachromosomal interaction was abolished in the *Kcnq1ot1 ZF-Sss1*–silenced cells (Fig. 3 C, lanes 3 and 4, left middle sections for three EcoRI ligated products: R1/R5, R2/R4, and R2/R5). Similarly, this long-range intrachromosomal interaction was lost in our other two models: the paternally inherited KvDMR1-deleted MEFs (Fig. 3 C, middle, lanes 3 and 4, R1/R5 and R2/R5) and the shRNA knockdown cells (Fig. 3 C, right, lanes 3 and 4, R1/R5 and R2/R5). Of note, the local interactions were not affected by *Kcnq1ot1* depletion. These data indicate that the lncRNA *Kcnq1ot1* is directly involved in and may be necessary for the maintenance of the long-range intrachromosomal loop between KvDMR1 and *Kcnq1* promoter.

To determine whether these local and long-distance interactions exist in an allele-specific manner, we used a polymorphism site PvuII near the *Kcnq1* promoter to distinguish the two parental alleles. In control and *Kcnq1ot1* knockout cells, local interactions within the *Kcnq1* promoter were biallelic (Fig. 3 D, right). However, in control cells, the long-range interaction between

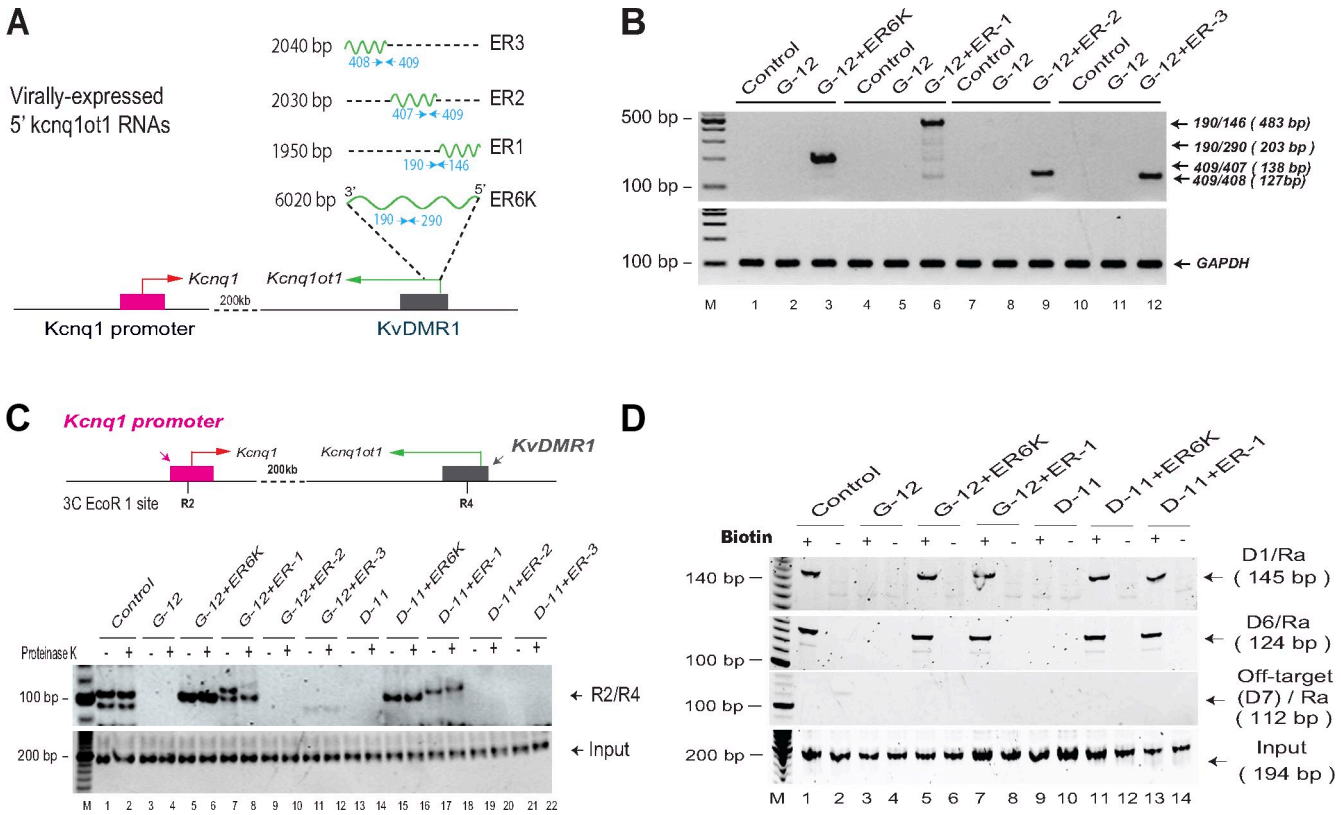

Figure 5. **The role of *Kcnq1ot1* lncRNA 5′ fragments is examined in shRNA-depleted cells.** (A) Schematic diagrams show the 5′ *Kcnq1ot1* fragments. Three 5′ subfragments were used in the functional mapping: ER6K (6,020 bp), ER1 (1,950 bp), ER2 (2,030 bp), and ER3 (2,040 bp). (B) RT-PCR shows the expression of exogenous constructs of 5′ *Kcnq1ot1* subfragment clones in the MBW2 fibroblast. RT-PCR product sizes: ER6K = 203 bp, ER1 = 483 bp, ER2 = 138 bp, and ER3 = 127 bp. (C) Long-range chromatin interactions are restored by ectopically expressed *Kcnq1ot1* subfragments. The chromatin loop between the *Kcnq1* promoter (R2) and KvDMR1 (R4) mediated by *Kcnq1ot1* lncRNA was detected by 3C. Control, normal MBW2 cells; D11 and G12, *Kcnq1ot1* shRNAs. (D) R3C confirms the interaction of the virally expressed 5′ *Kcnq1ot1* lncRNA subfragment (Ra) with the *Kcnq1* promoter (D1) and KvDMR1 (D6). M, 100-bp marker.

the *Kcnq1* promoter and KvDMR1 was monoallelic and was derived exclusively from the paternal allele (Fig. 3 D, left). These data show that the lncRNA *Kcnq1ot1* maintains the intrachromosomal *Kcnq1* promoter –KvDMR1 loop in an allele-specific manner.

Kcnq1ot1 lncRNA is required for the maintenance of *Kcnq1* and *Cdkn1c* imprinting

We then examined whether the abolition of the intrachromosomal loop between the *Kcnq1* promoter and KvDMR1 after *Kcnq1ot1* silencing would affect allelic expression of genes in the *Kcnq1* locus (Fig. 4 A). Using PCR, we detected monoallelic expression of *Kcnq1* in control and mock-transfected mouse fibroblast cells (Fig. 4 E, lanes 5 and 6); however, in cells that lack *Kcnq1ot1*, imprinting was lost (Fig. 4 E, lanes 1–4), and *Kcnq1* became biallelically expressed. Similarly, *Cdkn1c* also became biallelically expressed when *Kcnq1ot1* was silenced (Fig. 4 F, lanes 1–4). These data thus demonstrate the importance of the *Kcnq1ot1*-mediated intrachromosomal interaction in the maintenance of allelic expression in this imprinting locus.

Cd81 (Fig. 4 D) and *Osbp15* (Fig. 4 G), genes that are normally only imprinted in the placenta, were biallelically expressed in the control cells as well as in the cells that lacked *Kcnq1ot1*. Imprinting of the far upstream genes *Igf2* (Fig. 4 C) and *H19* (Fig. 4 B) was not altered, and there was no alteration in the DNA methylation of the *Igf2/H19* ICR (Fig. S3 D).

Restoration of intrachromosomal interaction by ectopic expression of 5′ *Kcnq1ot1* RNA

Next, we were interested in exploring the mechanism by which *Kcnq1ot1* noncoding RNA coordinates the long-range chromatin interaction in cis and, consequently, allelic regulation. We focused on the role of the 5′ *Kcnq1ot1* lncRNA in vivo by taking advantage of shRNA knockdown cells that are deficient in *Kcnq1ot1* lncRNA and that show an absence of the intrachromosomal interaction and the loss of genomic imprinting. To delineate the specific regions that interact with chromatin DNA, we cloned a 6-kb 5′ *Kcnq1ot1* fragment (ER6K) and three 2-kb subfragments (ER1, ER2, and ER3; Fig. 5 A) and virally expressed them in two shRNA knockdown cell clones (G-12 and D-11). The A-11 knockdown cell clone (Fig. 2 A) was excluded from this study as it covers a region that is very close to the 5′ *Kcnq1ot1* region. RT-PCR assay showed that these *Kcnq1ot1* fragments were expressed in virally transducted cells but not in the control cells (Fig. 5 B).

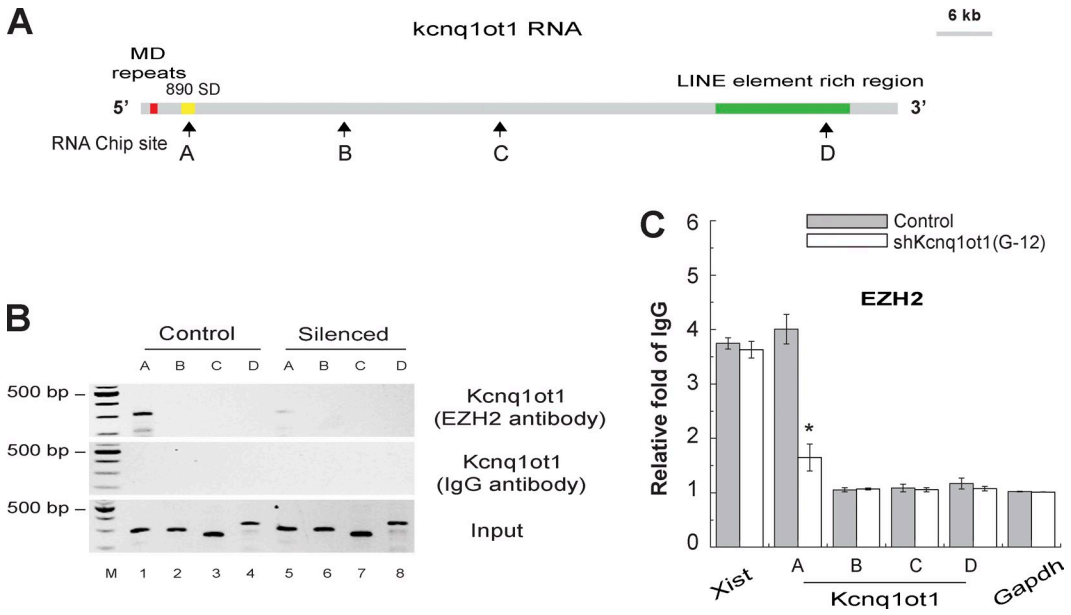

Figure 6. **Recruitment of histone methylase Ezh2 by *Kcnq1ot1* RNA.** (A) The schematic diagram shows the physical map of *Kcnq1ot1* RNA with conserved motifs. The letters mark the location of RNA ChIP-specific primers. A–D, lncRNA detection sites; SD, silencing domain. (B) Kcnq1ot1 shRNA knockdown alters Ezh2 binding to *Kcnq1ot1* RNA. Input, RNA collected before antibody precipitation. M, 100-bp marker. (C) Real-time PCR quantitates the Ezh2 interaction with specific regions of *Kcnq1ot1* RNA. ChIP data are presented as fold over IgG control, with IgG level set as 1. *Xsit* lncRNA was used as the positive control. *, $P < 0.05$ relative to *Kcnq1ot1* protein binding in the control. All data are presented as means ± SD of three independent experiments.

We found that the intrachromosomal interaction between the *Kcnq1* promoter and KvDMR1 was detected in wild-type controls (Fig. 5 C, lanes 1 and 2) and was lost in shRNA knockdown cells (Fig. 5 C, lanes 3 and 4). Ectopic expression of a 6-kb 5′ *Kcnq1ot1* lncRNA (ER6K) was sufficient to rescue the intrachromosomal interaction in two shRNA knockdown clones (G-12 and D-11; Fig. 5 C, lanes 5, 6, 15, and 16). A 2-kb subfragment (ER1) was also able to restore the majority, if not all, of this long-range DNA interaction (Fig. 5 C, lanes 7 and 17), indicating that this fragment covers a DNA interaction domain (DID) critical for maintaining long-distance intrachromosomal interaction. The other two downstream subfragments (ER2 and ER3), however, did not exhibit this function (Fig. 5 C, lanes 9, 11, 19, and 21). Using R3C, we confirmed that both the ectopically expressed ER6K and ER1 fragments directly interacted with the *Kcnq1* promoter (D1/Ra and D6/Ra; Fig. 5 D, lanes 5 and 7) and the KvDMR1 region (D6/Ra and D6/Ra; Fig. 5 D, lanes 11 and 13). No interactions were detected in the off-target control site (D7/Ra). Collectively, these data suggest that the virally expressed 6-kb *Kcnq1ot1* lncRNA binds to its target DNAs (*Kcnq1* promoter and KvDMR1) but not to an off-target site (D7) that is 10 kb away from the KvDMR1 (Fig. 1 B).

We also performed RNA FISH and DNA FISH assays simultaneously to examine this chromatin interaction. As previously described (Redrup et al., 2009), we detected the colocalization of the endogenous *Kcnq1ot1* RNA with the maternal *Kcnq1* chromatin DNA in MBW2 fibroblasts (Fig. S5 A). However, the viral 6-kb *Kcnq1ot1* lncRNA was abundantly expressed in shRNA knockdown cells, making it hard to detect the single molecule interaction of the viral lncRNA with *Kcnq1* chromatin DNA.

Kcnq1ot1 recruits EZH2 through its 5′-terminal domain

Next, we were interested in exploring trans-chromatin–modifying factors that coordinate the *Kcnq1ot1*-mediated long-range chromatin interaction and allelic regulation. For this purpose, we focused on PRC2. We first used chromatin RNA immunoprecipitation to examine whether *Kcnq1ot1* lncRNA recruits the methyltransferase EZH2, a component of PRC2, in guiding allelic gene regulation. The 5′ terminus of *Kcnq1ot1* contains an 890-bp silencing region (890 silencing domain; Mohammad et al., 2008) and a conserved repeat motif (MD1 repeats) region, whereas the 3′ terminus has a LINE (long interspersed nuclear element) element-rich region (Pandey et al., 2008). We used an anti-EZH2 antibody to immunoprecipitate chromatin complexes containing nuclear RNA. After digestion of genomic DNA and RT of RNA into cDNA, PCR was used to map the binding sites of *Kcnq1ot1* to EZH2 (Fig. 6 A). We found that in control cells, EZH2 interacted with the 890-bp silencing domain region at the 5′ terminus (A site) of *Kcnq1ot1* (Fig. 6 B, top, lane 1). No EZH2 interaction was detected at the central (B and C sites) or 3′-terminal regions (D site; Fig. 6 B, top, lanes 2–4). In *Kcnq1ot1*-silenced cells, the 5′-terminal interaction was lost (Fig. 6 B, top, lanes 5–8). Using the same approach, we also observed the loss of the EZH2 recruitment in the 5′ region of the lncRNA in cells in which the *Kcnq1ot1* was knocked down by G-12 shRNA (Fig. 6 C).

Kcnq1ot1 lncRNA guides allelic H3-K27 methylation at the Kcnq1 promoter

We then used chromatin immunoprecipitation (ChIP) to validate the recruitment of EZH2 to the promoter and KvDMR1 regions (Fig. 7 A). In control cells, EZH2 was enriched in the

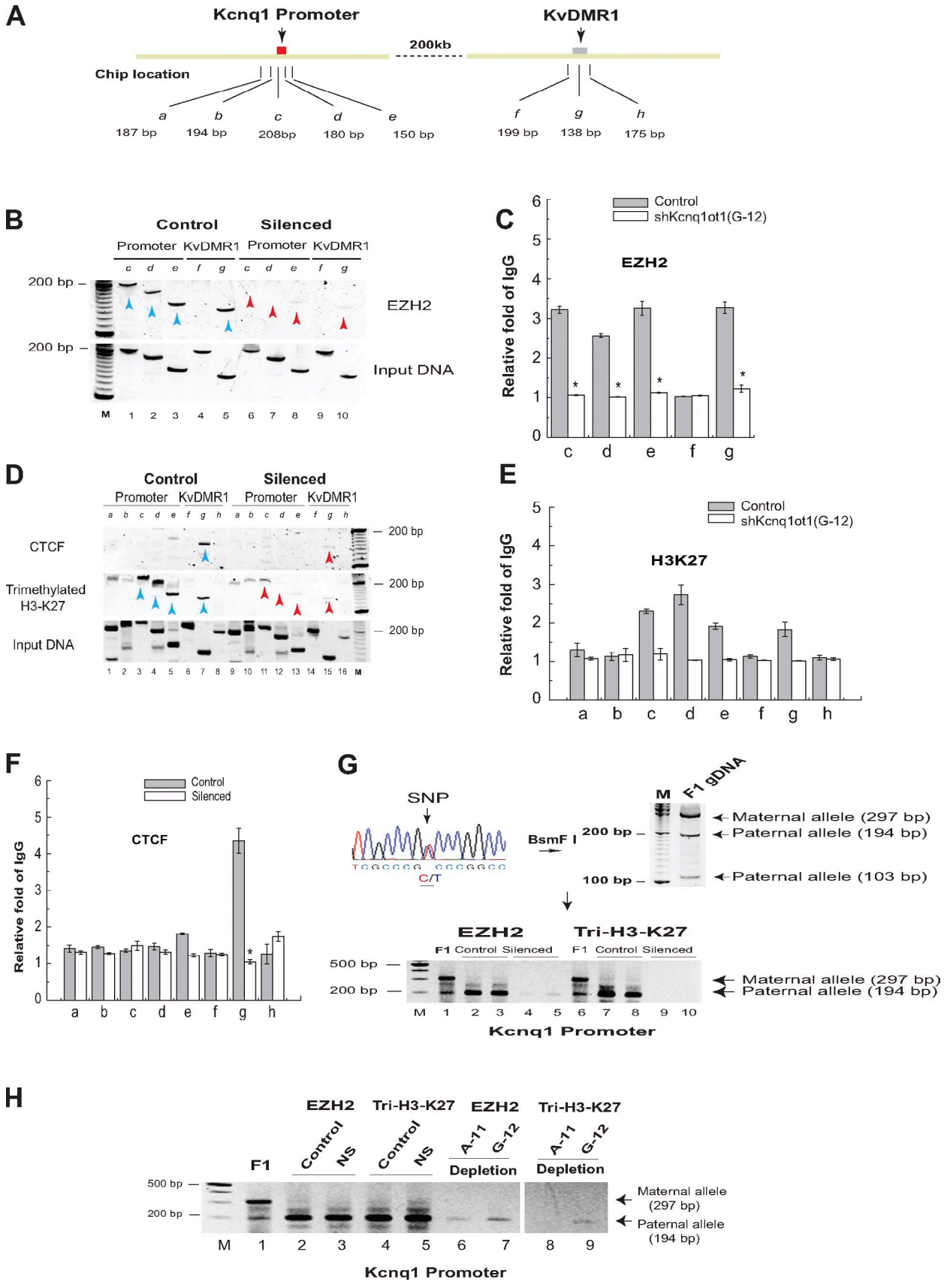

Figure 7. ***Kcnq1ot1* lncRNA guides histone H3-K27 methylation in the *Kcnq1* promoter.** (A) Schematic diagram shows the size of H3-K27 ChIP products in the *Kcnq1* imprinting domain. The letters (a–e) mark the location of the ChIP-specific primers. (B–F) ChIP assay detects the recruitment of Ezh2, CTCF, and histone H3-K27 methylation at the *Kcnq1* promoter in *Kcnq1ot1*-silenced cells (B, D, and F) and shRNA-depleted cells (C and E). Cross-linked DNA–protein

Kcnq1 promoter and KvDMR1 regions (Fig. 7 B, top and middle, lanes 1–5, blue arrows); however, in *Kcnq1ot1*-silenced cells, there was far less EZH2 binding at those regions (Fig. 7 B, top and middle, lanes 6–10, red arrows). Similarly, the binding of EZH2 to the promoter and KvDMR1 was lost in the *Kcnq1ot1* shRNA knockdown cells (Fig. 7 C). Together, these data suggest that *Kcnq1ot1* lncRNA must be present to recruit PRC2 to the targeted DNA regions.

We then examined whether the recruitment of the PRC2 complex would induce the H3-K27 methylation suppression mark in the *Kcnq1* promoter. In control cells, we observed H3-K27 hypermethylation at the *Kcnq1* promoter and KvDMR1 region (Fig. 7 D, middle, lanes 1–8, blue arrows). In cells that lack *Kcnq1ot1*, in contrast, there was a decrease in H3-K27me3 in the promoter (Fig. 7 D, middle, lanes 9–16, red arrows), consistent with a loss of EZH2 binding. In support of this finding, we also observed that H3-K27 methylation suppression was abolished in the *Kcnq1ot1* shRNA–knocked down cells (Fig. 7 E).

We also examined CTCF binding in these regions. In control cells, CTCF bound only at the KvDMR1 region and not at the *Kcnq1* promoter (Fig. 7 D, top, lane 7, blue arrow). In *Kcnq1ot1* methylation silenced cells, no CTCF binding was detected (Fig. 7, D and F). These data suggest that CTCF may not directly participate in this long-distance intrachromosomal interaction. Loss of CTCF binding may simply be related to the exclusion of CTCF after DNA methylation at the CTCF site in KvDMR1.

To identify whether EZH2 binding and histone H3-K27 methylation at the *Kcnq1* promoter is allele specific, we sequenced the immunoprecipitated DNA. Using a BsmFI SNP site in the *Kcnq1* promoter to distinguish the parental alleles, we found that EZH2 binding and H3-K27 methylation occurred in a paternal allele-specific manner (Fig. 7 G). However, this parent-specific EZH2 binding and H3-K27 methylation did not occur in shRNA-mediated *Kcnq1ot1* depletion cells (Fig. 7 H). These data thus suggest that *Kcnq1ot1* lncRNA guides allelic H3-K27 methylation at the *Kcnq1* promoter to induce the allelic imprinting.

Discussion

We have begun to unravel the mechanisms by which the lncRNA *Kcnq1ot1* regulates allelic expression of a cluster of genes in the *Kcnq1* imprinting domain. Using two complementary approaches, we demonstrate that *Kcnq1ot1* lncRNA interacts directly with chromatin to form a 200-kb intrachromosomal loop between the downstream *Kcnq1* promoter and the KvDMR1where the *Kcnq1ot1* promoter is located.

First, we developed an R3C method to examine this RNA–chromatin DNA interaction. The *Kcnq1ot1* lncRNA that was interacting with chromatin was reverse transcribed into double-stranded cDNA. After restriction enzyme digestion, the sticky ends from the *Kcnq1ot1* cDNA and the interacting chromatin DNA were ligated, and the chimeric products were identified after PCR amplification. To confirm this lncRNA–DNA interaction, we also used a ChOP method (Mariner et al., 2008; Pandey et al., 2008) to detect enrichment of *Kcnq1ot1* lncRNA at the *Kcnq1* promoter and KvDMR1 regions. The *Kcnq1ot1* lncRNA was pulled down with biotin-labeled antisense oligonucleotides, and the interacting chromatin DNA was amplified by PCR primers. Using these complementary techniques, we demonstrate that *Kcnq1ot1* lncRNA interacts with chromatin DNA through its 5′-terminal region, which has been termed the silencing domain (Fig. S4). The R3C methodology can be used to examine specific RNA–DNA interactions throughout the genome.

To demonstrate the role of the lncRNA in regulating this imprinted region, we inhibited *Kcnq1ot1* lncRNA synthesis by methylating the CpG1 island on the paternal allele, thereby silencing the lncRNA's promoter. This was achieved by constructing a fusion protein containing the ZF DNA binding portion of CTCF connected to Sss1, a DNA methyltransferase. This protein binds to CTCF binding sites and has the ability to methylate nearby CpG moieties in some but not all genes (Zhang et al., 2011). In cells transfected with a lentivirus delivering this fusion construct, we demonstrated that CpG1 was methylated by this fusion protein. Using this novel approach, we showed that the expression of *Kcnq1ot1* was greatly decreased in these cells and that no interactions of this lncRNA at KvDMR1 or the *Kcnq1* promoter could be detected. These findings were validated in a KvDMR1 knockout mutant mouse cell line (Fig. 2 E; Fitzpatrick et al., 2002) as well as in an shRNA-mediated RNAi depletion model (Fig. 2 F).

The interaction of *Kcnq1ot1* with the KvDMR1 and with *Kcnq1* loci that are 200 kb apart suggests the presence of a DNA loop that juxtaposes the two regulatory regions (Murrell et al., 2004). Using a standard 3C approach, we showed that the two regions do in fact interact with each other but that this interaction no longer occurs when the *Kcnq1ot1* expression is silenced by targeted DNA methylation or by shRNA or is knocked out in the paternally inherited mutant fetal mice (Fig. 3 C), indicating that this lncRNA is a necessary component of this three-dimensional structure. The suppression of *Kcnq1ot1* leads to loss of imprinting in this region, as well, suggesting that this long-range chromatin interaction is required for allele-specific gene expression.

complexes were immunoprecipitated with antiserum against Ezh2, CTCF, or trimethyl–H3-K27 (mK27) followed by PCR amplification with specific primers. Input, genomic DNA collected before antibody precipitation. (C–F) The immunoprecipitated DNA was quantitated by real-time PCR and was calculated as fold of the *Kcnq1ot1*-IgG level. Arrowheads: red (control); blue (silenced). Results are shown as the means (bars) ± SD of three independent experiments. *, $P < 0.05$ as compared with the control. (G) *Kcnq1ot1* silencing abolishes allele-specific EZH2 recruitment and histone H3-K27 methylation at the *Kcnq1* promoter. After PCR, the two parental alleles were distinguished by BsmFI polymorphic restriction enzyme. (H) *Kcnq1ot1* shRNA knockdown alters allelic EZH2 recruitment and histone H3-K27 methylation at the *Kcnq1* promoter. F1, control genomic DNA (gDNA) digested by BsmFI. Control, untreated cells; NS, nonsilencing random nontargeting shRNA control; A-11 and G-11, Kcnq1ot1 lncRNA–targeted shRNAs. Note that H3-K27 methylation was not affected by shRNA knockdown. M, 100-bp marker.

Chromatin loops are built and stabilized with a host of nuclear proteins. CTCF has been implicated in numerous long-range interactions, and as a result, it has been called the master weaver of the genome (Phillips and Corces, 2009). CTCF regulates allelic expression of mouse *Igf2* by forming a long-range intrachromosomal loop (Murrell et al., 2004; Li et al., 2008; Qiu et al., 2008). Although CTCF binds to KvDMR1, it does not bind to the *Kcnq1* promoter, suggesting that CTCF is not involved in the loop formation at the *Kcnq1* locus. In this study, however, we have identified a totally novel, RNA-based mechanism for organizing intrachromosomal looping. The R3C data show that only the 5′ terminus of the *Kcnq1ot1* lncRNA is necessary for establishing the *Kcnq1ot1*–DNA interaction. By expressing fragments of the 5′ end of *Kcnq1ot1* ectopically, we have localized the DID to a ∼6-kb region (Fig. 5). This DID domain binds to both the *Kcnq1* promoter and KvDMR1 DNAs and helps establish a long-distance intrachromosomal interaction.

Although the precise mechanisms governing genomic imprinting are not fully understood, it is now clear that each imprinted chromosomal domain contains its ICR, in which the imprinting signal coordinates the imprinting of multiple genes over hundreds of kilobases of DNA (Leighton et al., 1995; Wutz et al., 1997; Thorvaldsen et al., 1998; Fitzpatrick et al., 2002). In the *Kcnq1* imprinting domain, the ICR has been identified as a conserved, differentially methylated CpG island within intron 10 of *Kcnq1* in both human (De Marzo et al., 1999; Lee et al., 1999) and mouse (Smilinich et al., 1999), and deletion of EZH2 supports a role for EZH2 in imprinted repression and higher-order genomic contraction along the entire paternal *Kcnq1* cluster (Terranova et al., 2008). In this case, however, it is not the ZF protein CTCF but rather the nuclear noncoding RNA *Kcnq1ot1* that conveys the imprinting message from the ICR to the *Kcnq1* promoter, which is 200 kb away (Fig. S5 B).

Many questions remain regarding the mechanisms underlying the formation and maintenance of this intrachromosomal looping. Our data are consistent with a model in which the *Kcnq1ot1* lncRNA may function as a molecular hinge, using different segments of the 5′-terminal region to link the paternal *Kcnq1* promoter and KvDMR1 DNAs together and scaffold a long-range intrachromosomal loop (Fig. S5 B). With this spatial proximity, the imprinting signal in the KvDMR1 can be delivered to the *Kcnq1* promoter. The lncRNA then recruits PRC2 to the target *Kcnq1* promoter, where allele-specific histone H3-K27 methylation turns off expression of the paternal *Kcnq1*. On the maternal chromosome or in Kcnq1ot1-deficient cells, failure to form an intrachromosomal loop leads to biallelic expression of Kcnq1. However, it should be noted that the chromatin DNA in imprinted loci, such as the *Kcnq1* region, is highly condensed. The compaction of the silenced chromatin may also increase the proximity of the lncRNA with the Kcnq1 promoter as detected by R3C. Further studies are needed to validate the role of *Kcnq1ot1* lncRNA in the formation of an intrachromosomal loop by excluding the involvement of condensed chromatin.

In summary, formation of intrachromosomal looping may constitute a common mechanism underlying the long-range cis-regulation of clustered genes. We present a model whereby the *Kcnq1ot1* lncRNA participates in long-distance chromatin interaction through its 5′-terminal region. EZH2 is then recruited to the *Kcnq1* promoter by the nuclear factor interaction domain of the lncRNA (Fig. S5 B). We suggest that the *Kcnq1ot1* lncRNA acts as a scaffold molecule to juxtapose the *Kcnq1* promoter region to the KvDMR1 region on the paternal chromosome. This concept is supported by the fact that the long-range chromosomal interaction conformation was lost after the silencing of *Kcnq1ot1* by targeted DNA methylation. This long-range intrachromosomal interaction is essential for the maintenance of imprinting of genes in the *Kcnq1* region. Thus, long-range chromatin interactions may play an important role in the allelic regulation of gene expression and genomic imprinting. Because many imprinted genes have noncoding RNAs associated with them, it is likely that these lncRNAs may play an important role in regulating chromatin structure to direct gene expression (Spitale et al., 2011).

Materials and methods

Cell lines

Mouse fibroblast MBW2 cells were cultured from an F1 newborn mouse derived from breeding an *M. spretus* male with a C57B/6 female in our laboratory as previously described (Hu et al., 1996, 1997). These cells maintain normal monoallelic expression for imprinted genes (Hu and Hoffman, 2001), including *Kcnq1ot1* and *Kcnq1*. 293SF-PacLV cells were provided by R. Gilbert from the National Research Council (Ottawa, Ontario, Canada) and were cultured as previously described (Broussau et al., 2008). The *Kcnq1ot1* knockout MEFs were cultured from embryonic day 15.5–16.5 fetuses, which carry the deletion of a 2.8-kb KvDMR1 fragment containing the *Kcnq1ot1* promoter (Fitzpatrick et al., 2002). Both MBW2 and *Kcnq1ot1* knockout MEFs were maintained in DMEM supplemented with 10% FBS, 100 U/ml penicillin, and 100 µg/ml streptomycin.

Methylation targeting vector construction

The CTCF analogue ZF-*Sss1* was synthesized as previously described (Zhang et al., 2011). In brief, *Sss1* DNA methyltransferase DNA was amplified from *Spiroplasma monobiae* strain MQ1 (33825; ATCC) genomic DNA, and the cDNA fragment encoding the CTCF ZF domain was generated from the pOBT7-CTCF vector by PCR amplification. These two DNA fragments were then linked by SV40 NLS and a short linker sequence to produce the ZF-*Sss1* construct, which was then cloned into the NheI–BamH sites in pCDH-CMV-MCS-EF1-Puro lentivirus vector (System Biosciences, Inc.).

Lentiviral transduction

The lentiviruses were generated in 293SF-PacLV packing cells that stably express VSV-G, Gag-Pol, and Rev packaging genes (Broussau et al., 2008). In brief, cells were transfected with the lentiviral expression vector. 12 h after transfection, culture medium was replaced by fresh medium containing 1 µg/µl doxycycline and 30 µg/µl cumate. The virus-containing supernatants were collected at 48 and 72 h. The pooled viral supernatants were filtered through a 0.45-mm filter, concentrated by a PEG-it kit (System Biosciences, Inc.), and stored at −80°C. Mouse MBW2 fibroblasts were seeded at 1.0×10^5 cells per well in 6-well plates 24 h before transduction. The medium was replaced with virus-containing supernatant containing 5 mg/ml polybrene (Sigma-Aldrich) and incubated overnight. 24 h after transduction, the virus-containing medium was replaced with fresh medium. 4 d later, the infected cells were harvested by trypsinization and replated on a new 100-mm dish. When cell confluence reached 20–30%, the culture medium was replaced by fresh medium containing 1 µg/µl puromycin for colony selection. The medium was changed every 3–4 d. After selection, colonies were chosen and expanded for further analyses.

DNA methylation analysis

Total nucleic acids were extracted from normal and transformed MBW2. As previously described (Yao et al., 2003; Chen et al., 2006), total nucleic acid was treated with sodium bisulfate, and PCR was performed using DNA methylation–specific primers designed for CTCF binding sites (Table S1). To examine the status of DNA methylation in every CpG site in the two

CTCF binding regions of KvDMR1, the amplified PCR DNAs were cloned into the TA vector (Invitrogen) and sequenced. DNA in the third CTCF binding site of the *Igf2/H19* differentially methylated region was amplified and separated by BstUI to determine methylated and unmethylated DNAs.

3C

The 3C assay was performed as previously described (Dekker, 2006; Zhang et al., 2011). In brief, cells were cross-linked with 2% formaldehyde and lysed with cell lysis buffer. An aliquot of nuclei (2×10^6) was digested with 800 U EcoRI at 37°C overnight. Chromatin DNA was diluted with ligation buffer (New England Biolabs, Inc.) and ligated with 4,000 U T4 DNA ligase. DNA was extracted with phenol–chloroform and used for PCR amplification using primers in Table S2.

R3C

Cells were fixed with 2% formaldehyde and lysed with cell lysis buffer (10 mM Tris, pH 8.0, 10 mM NaCl, 0.2% NP-40, and protease inhibitors). Nuclei were suspended in 100 µl cDNA synthesis buffer in the presence of 0.3% SDS. After incubated at 37°C for 1 h, Triton X-100 was added to a final concentration of 1.8% to sequester the SDS. The first-stand cDNAs were synthesized in an 80-µl reaction (3 µl random primer, 3 µl gene-specific primer, 10 mM deoxy-ATP [1.5 µl], 10 mM deoxy-GTP [1.5 µl], 10 mM deoxy-TTP [1.5 µl], 0.4 mM dCTP-biotin [3.75 µl], 10 mM dCTP [1.35 µl], 6 µl RT enzyme, 6 µl RNase inhibitors, 0.1 M DTT [6 µl], and 18 µl 5× cDNA synthesis buffer). The second-strand cDNA was synthesized in a 150-µl reaction using cDNA Synthesis kit (Agilent Technologies). A 50-µl aliquot was digested with 600 U EcoRI at 37°C overnight. After stopping the reaction by adding 1.6% SDS and incubating the mixture at 65°C for 20 min, chromatin DNA was diluted with NEB ligation reaction buffer and then ligated with 4,000 U T4 DNA ligase at 16°C for 4 h (final DNA concentration of 2.5 µg/ml). After treatment with 10 mg/ml proteinase K at 65°C overnight to reverse cross-links and with 0.4 µg/ml RNase A for 30 min at 37°C, DNA was extracted with phenol–chloroform, ethanol precipitated, and then purified by streptavidin beads (Invitrogen). Purified DNA was used for PCR amplification using primers in Table S3. Synthetic oligonucleotides were used as positive controls. The R3C products were cloned into pJet cloning vector (Thermo Fisher Scientific) and sequenced to confirm the lncRNA–chromatin DNA interaction.

R3C control assays

We first examined whether the biotin-labeled DNA fragments were able to be digested by restriction enzyme EcoRI. Biotinylated DNAs were prepared by PCR amplification of plasmid vectors pCDH1 (System Biosciences, Inc.) and pEGFP-C1 (Takara Bio Inc.) in the presence of 1 µl of 0.4-mM dCTP-biotin (Invitrogen). Amplified PCR products were digested by EcoRI enzyme.

We then examined whether the cross-linked chromatin RNA were able to be reverse transcribed. As described in the previous R3C section, the EcoRI-digested sample was immunoprecipitated by 5–10 µg histone H3 antibody (EMD Millipore), pulled down by protein G magnetic beads (EMD Millipore), and pretreated by DNase I for 30 min at 37°C. The first-stand cDNA was synthesized using a cDNA kit (Agilent Technologies). After cross-linking reversal, PCR was used to examine the synthesized cDNA by specific PCR primers: *pKcnq1* (H6/H9) and *Kcnq1ot1* (H145/H146).

Finally, we examined whether the second-strand cDNA can be synthesized on cross-linked chromatin lncRNA. The first-stand cDNA was synthesized on the anti–histone H3 pulled down protein G magnetic beads using a strand-specific RT primer #R4A (Table S2). The second-strand cDNA was synthesized using the cDNA kit (Agilent Technologies) in the presence of 3.75 µl of 0.4-mM dCTP-biotin. After washing beads three to five times with 500 µl PBS buffer with 0.1% Tween 20, the synthesized second-strand cDNA was released from the beads and purified by biotin-streptavidin pull-down (Invitrogen). PCR reactions were performed to distinguish double-strand cDNA and genomic DNA: double-strand cDNA (H147/H148) and genomic DNA (H145/H263; H263 sequence, 5′-TAGAGATTCGGGTCTGGAGCCGACT-3′).

ChIP

ChIP assays were performed as described previously (Zhang et al., 2011). In brief, cells were fixed with 1% formaldehyde and sonicated on ice with a Branson sonicator. 150 µl of sonicated chromatin was immunoprecipitated using 2–5 µl of specific antiserum and 60 µl protein G–agarose. Antibodies to SMC1, CTCF, SUZ12, Ezh2, trimethyl–H3-K27 (lysine 27 of histone H3), and dimethyl–H3-K9 (lysine 9 of histone H3) were obtained from Abcam. The DNA was extracted for PCR using primers listed in Table S4.

RNA ChIP

RNA immunoprecipitation assays were performed as described by Rinn et al. (2007). In brief, cells were fixed with 1% formaldehyde, treated with DNase I, and sonicated using a sonicator (Vibra-Cell VCX130; Sonics & Materials, Inc.). Sonicated samples were immunoprecipitated with protein G–agarose, and antibodies were raised against SMC1, SUZ12, Ezh2, and IgG (Abcam). The precipitated RNA was released, and cDNA was synthesized. After proteinase K treatment, cDNA was precipitated, and *Kcnq1ot1* and *GAPDH* were detected by semiquantitative PCR using the primers listed in Table S5.

ChOP

The ChOP assays were performed according to published protocol (Mariner et al., 2008; Pandey et al., 2008). In brief, nuclei were lysed in nuclei lysis buffer, sonicated, incubated with 50 pmol biotin-labeled antisense oligonucleotide, and pulled down according to the manufacturer's protocol (Invitrogen). The enrichment of *Kcnq1ot1*-interacting genomic DNA regions was analyzed by PCR using primers derived from the *Kcnq1* domain (Table S6).

Determination of genomic imprinting

Total RNA extraction and cDNA synthesis were performed as previously described (Hu et al., 1995). Allelic expression of *Kcnq1*, *Cdkn1c*, *Osbpl5*, *and Cd81* was examined by PCR in cDNA samples using primers specific for polymorphic restriction enzymes. Allelic expression of *Igf2* and *H19* was assessed by polymorphic restriction enzyme DpnII and FoxI, respectively. PCR primers used to assess allelic expression are listed in Table S7.

RNA extraction and RT-PCR analysis

Total RNA was extracted by TRI Reagent (Sigma-Aldrich), and cDNA was synthesized using RNA RT. PCR was performed using KlenTaq I mix, and amplified PCR products were quantified and normalized using *GAPDH* as a control (Tables S5 and S8).

shRNA lentivirus and selection

Kcnq1ot1, *SMC1*, *Kcnq1*, *H19*, and *Nespas* shRNA constructs, and verified nonsilencing shRNA were purchased from Thermo Fisher Scientific (Table S9). Selection was performed with 3 µg/ml puromycin, and the clones were screened for GFP expression.

5′-end *Kcnq1ot1* constructs

Four fragments of the 5′ terminus of *Kcnq1ot1*, including a full 6-kb sequence (ER6K; 6,020 bp), ER1 (1,950 bp), ER2 (2,030 bp), and ER3 (2,040 bp) sequences, were amplified from bacterial artificial chromosome (BAC) clone RP23-400C11 and cloned into the NheI–NotI sites in pCDH-CMV-MCS-EF1-Puro lentivirus vector (Table S10).

RNA–DNA FISH

Cells were fixed with 4% formaldehyde/10% acetic acid and stored overnight in 70% ethanol. For RNA FISH, fluorescence-labeled single-strand DNA probes (Stellaris) were synthesized by Biosearch Technologies and were hybridized according to manufacturer's protocol. To increase stability of RNA foci, RNA signals were detected with a tyramide–Alexa Fluor 488 signal amplification kit (Invitrogen). For DNA FISH, BAC probes labeled with DNP-dUTP were denatured and hybridized overnight. Detection of BAC probes was performed with rabbit anti-DNP (Invitrogen) and secondary goat anti–rabbit conjugated to Alexa Fluor 594. After labeling, fluorescence was detected using a microscope (BX41; Olympus). Optical sections of 0.2 µm were collected with SlideBook 5.0 (Intelligent Imaging Innovations, Inc.).

Statistical analysis

All experiments were performed in triplicate, and the data are expressed as means ± SD. The comparative threshold cycle method was applied in the quantitative real-time RT-PCR assay according to the ΔΔ threshold cycle method.

Online supplemental material

Fig. S1 shows the control assays that validate each critical step in the R3C approach (Table S8). Fig. S2 shows the data of negative controls for R3C method. Fig. S3 demonstrates shRNA knockdown of *Kcnq1ot1* lncRNA. Fig. S4 validates the *Kcnq1ot1* lncRNA–chromatin DNA interaction by ChOP assay. Fig. S5 shows the interaction of *Kcnq1ot1* lncRNA with *Kcnq1* promoter DNA by RNA–DNA FISH and the proposed model for *Kcnq1ot1* lncRNA-mediated *Kcnq1* imprinting. Table S1 shows primers used for the DNA methylation assay. Table S2 shows primers used for 3C at the *Kcnq1* locus. Table S3 shows primers used for R3C at the *Kcnq1* locus.

Table S4 shows primers used for the ChIP assay. Table S5 shows primers used for the RNA ChIP assay. Table S6 shows oligonucleotides and PCR primers used for the ChOP assay. Table S7 shows primers for allelic expression of imprinted genes. Table S8 shows primers used to amplify DNA fragments with the EcoRI site. Table S9 shows primers and shRNA sets for RNAi. Table S10 shows primers for the *Kcnq1ot1 5′*-end deletion assay. Online supplemental material is available at http://www.jcb.org/cgi/content/full/jcb.201304152/DC1.

We thank the Protein and Nucleic Acid Facility at the Stanford University School of Medicine for oligonucleotide synthesis.

This work was supported by a California Institute of Regenerative Medicine grant (RT2-01942), Ja ilin International Collaboration grant (20120720), and a Natural Science Foundation of China grant (81272294) to J.-F. Hu; the Medical Research Service of the Department of Veterans Affairs to A.R. Hoffman; the National Natural Science Foundation of China grant (81172323) and the Strategic Priority Research Program of the Chinese Academy of Sciences grant (XDA01040411) to S. Ge; and a Shanghai Leading Academic Discipline Project grant (S30205) to X. Fan. H. Zhang is an Early Career Scientist of the Shanghai JiaoTong University School of Medicine.

The authors have no conflicting financial interests.

Submitted: 23 April 2013
Accepted: 25 November 2013

References

Broussau, S., N. Jabbour, G. Lachapelle, Y. Durocher, R. Tom, J. Transfiguracion, R. Gilbert, and B. Massie. 2008. Inducible packaging cells for large-scale production of lentiviral vectors in serum-free suspension culture. *Mol. Ther.* 16:500–507. http://dx.doi.org/10.1038/sj.mt.6300383

Chen, H.L., T. Li, X.W. Qiu, J. Wu, J.Q. Ling, Z.H. Sun, W. Wang, W. Chen, A. Hou, T.H. Vu, et al. 2006. Correction of aberrant imprinting of IGF2 in human tumors by nuclear transfer-induced epigenetic reprogramming. *EMBO J.* 25:5329–5338. http://dx.doi.org/10.1038/sj.emboj.7601399

De Marzo, A.M., V.L. Marchi, E.S. Yang, R. Veeraswamy, X. Lin, and W.G. Nelson. 1999. Abnormal regulation of DNA methyltransferase expression during colorectal carcinogenesis. *Cancer Res.* 59:3855–3860.

Dekker, J. 2006. The three 'C's of chromosome conformation capture: controls, controls, controls. *Nat. Methods*. 3:17–21. http://dx.doi.org/10.1038/nmeth823

Dekker, J., K. Rippe, M. Dekker, and N. Kleckner. 2002. Capturing chromosome conformation. *Science*. 295:1306–1311. http://dx.doi.org/10.1126/science.1067799

Fitzpatrick, G.V., P.D. Soloway, and M.J. Higgins. 2002. Regional loss of imprinting and growth deficiency in mice with a targeted deletion of KvDMR1. *Nat. Genet.* 32:426–431. http://dx.doi.org/10.1038/ng988

Fitzpatrick, G.V., E.M. Pugacheva, J.Y. Shin, Z. Abdullaev, Y. Yang, K. Khatod, V.V. Lobanenkov, and M.J. Higgins. 2007. Allele-specific binding of CTCF to the multipartite imprinting control region KvDMR1. *Mol. Cell. Biol.* 27:2636–2647. http://dx.doi.org/10.1128/MCB.02036-06

Golding, M.C., L.S. Magri, L. Zhang, S.A. Lalone, M.J. Higgins, and M.R. Mann. 2011. Depletion of Kcnq1ot1 non-coding RNA does not affect imprinting maintenance in stem cells. *Development*. 138:3667–3678. http://dx.doi.org/10.1242/dev.057778

Hu, J.F., and A.R. Hoffman. 2001. Examining histone acetylation at specific genomic regions. *Methods Mol. Biol.* 181:285–296.

Hu, J.F., T.H. Vu, and A.R. Hoffman. 1995. Differential biallelic activation of three insulin-like growth factor II promoters in the mouse central nervous system. *Mol. Endocrinol.* 9:628–636. http://dx.doi.org/10.1210/me.9.5.628

Hu, J.F., T.H. Vu, and A.R. Hoffman. 1996. Promoter-specific modulation of insulin-like growth factor II genomic imprinting by inhibitors of DNA methylation. *J. Biol. Chem.* 271:18253–18262. http://dx.doi.org/10.1074/jbc.271.30.18253

Hu, J.F., T.H. Vu, and A.R. Hoffman. 1997. Genomic deletion of an imprint maintenance element abolishes imprinting of both insulin-like growth factor II and H19. *J. Biol. Chem.* 272:20715–20720. http://dx.doi.org/10.1074/jbc.272.33.20715

Kanduri, C. 2011. Kcnq1ot1: a chromatin regulatory RNA. *Semin. Cell Dev. Biol.* 22:343–350. http://dx.doi.org/10.1016/j.semcdb.2011.02.020

Lee, J.T. 2012. Epigenetic regulation by long noncoding RNAs. *Science*. 338:1435–1439. http://dx.doi.org/10.1126/science.1231776

Lee, M.P., M.R. DeBaun, K. Mitsuya, H.L. Galonek, S. Brandenburg, M. Oshimura, and A.P. Feinberg. 1999. Loss of imprinting of a paternally expressed transcript, with antisense orientation to KVLQT1, occurs frequently in Beckwith-Wiedemann syndrome and is independent of insulin-like growth factor II imprinting. *Proc. Natl. Acad. Sci. USA*. 96:5203–5208. http://dx.doi.org/10.1073/pnas.96.9.5203

Leighton, P.A., R.S. Ingram, J. Eggenschwiler, A. Efstratiadis, and S.M. Tilghman. 1995. Disruption of imprinting caused by deletion of the H19 gene region in mice. *Nature*. 375:34–39. http://dx.doi.org/10.1038/375034a0

Li, T., J.F. Hu, X. Qiu, J. Ling, H. Chen, S. Wang, A. Hou, T.H. Vu, and A.R. Hoffman. 2008. CTCF regulates allelic expression of Igf2 by orchestrating a promoter-polycomb repressive complex 2 intrachromosomal loop. *Mol. Cell. Biol.* 28:6473–6482. http://dx.doi.org/10.1128/MCB.00204-08

Mancini-DiNardo, D., S.J. Steele, R.S. Ingram, and S.M. Tilghman. 2003. A differentially methylated region within the gene Kcnq1 functions as an imprinted promoter and silencer. *Hum. Mol. Genet.* 12:283–294. http://dx.doi.org/10.1093/hmg/ddg024

Mariner, P.D., R.D. Walters, C.A. Espinoza, L.F. Drullinger, S.D. Wagner, J.F. Kugel, and J.A. Goodrich. 2008. Human Alu RNA is a modular transacting repressor of mRNA transcription during heat shock. *Mol. Cell*. 29:499–509. http://dx.doi.org/10.1016/j.molcel.2007.12.013

Mohammad, F., R.R. Pandey, T. Nagano, L. Chakalova, T. Mondal, P. Fraser, and C. Kanduri. 2008. Kcnq1ot1/Lit1 noncoding RNA mediates transcriptional silencing by targeting to the perinucleolar region. *Mol. Cell. Biol.* 28:3713–3728. http://dx.doi.org/10.1128/MCB.02263-07

Murakami, K., M. Oshimura, and H. Kugoh. 2007. Suggestive evidence for chromosomal localization of non-coding RNA from imprinted LIT1. *J. Hum. Genet.* 52:926–933. http://dx.doi.org/10.1007/s10038-007-0196-4

Murrell, A., S. Heeson, and W. Reik. 2004. Interaction between differentially methylated regions partitions the imprinted genes Igf2 and H19 into parent-specific chromatin loops. *Nat. Genet.* 36:889–893. http://dx.doi.org/10.1038/ng1402

Nagano, T., and P. Fraser. 2011. No-nonsense functions for long noncoding RNAs. *Cell*. 145:178–181. http://dx.doi.org/10.1016/j.cell.2011.03.014

Pandey, R.R., T. Mondal, F. Mohammad, S. Enroth, L. Redrup, J. Komorowski, T. Nagano, D. Mancini-Dinardo, and C. Kanduri. 2008. Kcnq1ot1 antisense noncoding RNA mediates lineage-specific transcriptional silencing through chromatin-level regulation. *Mol. Cell*. 32:232–246. http://dx.doi.org/10.1016/j.molcel.2008.08.022

Paulsen, M., T. Khare, C. Burgard, S. Tierling, and J. Walter. 2005. Evolution of the Beckwith-Wiedemann syndrome region in vertebrates. *Genome Res.* 15:146–153. http://dx.doi.org/10.1101/gr.2689805

Phillips, J.E., and V.G. Corces. 2009. CTCF: master weaver of the genome. *Cell*. 137:1194–1211. http://dx.doi.org/10.1016/j.cell.2009.06.001

Prasanth, K.V., and D.L. Spector. 2007. Eukaryotic regulatory RNAs: an answer to the 'genome complexity' conundrum. *Genes Dev.* 21:11–42. http://dx.doi.org/10.1101/gad.1484207

Qiu, X., T.H. Vu, Q. Lu, J.Q. Ling, T. Li, A. Hou, S.K. Wang, H.L. Chen, J.F. Hu, and A.R. Hoffman. 2008. A complex deoxyribonucleic acid looping configuration associated with the silencing of the maternal Igf2 allele. *Mol. Endocrinol.* 22:1476–1488. http://dx.doi.org/10.1210/me.2007-0474

Redrup, L., M.R. Branco, E.R. Perdeaux, C. Krueger, A. Lewis, F. Santos, T. Nagano, B.S. Cobb, P. Fraser, and W. Reik. 2009. The long noncoding RNA Kcnq1ot1 organises a lineage-specific nuclear domain for epigenetic gene silencing. *Development*. 136:525–530. http://dx.doi.org/10.1242/dev.031328

Rinn, J.L., M. Kertesz, J.K. Wang, S.L. Squazzo, X. Xu, S.A. Brugmann, L.H. Goodnough, J.A. Helms, P.J. Farnham, E. Segal, and H.Y. Chang. 2007. Functional demarcation of active and silent chromatin domains in human HOX loci by noncoding RNAs. *Cell*. 129:1311–1323. http://dx.doi.org/10.1016/j.cell.2007.05.022

Smilinich, N.J., C.D. Day, G.V. Fitzpatrick, G.M. Caldwell, A.C. Lossie, P.R. Cooper, A.C. Smallwood, J.A. Joyce, P.N. Schofield, W. Reik, et al. 1999. A maternally methylated CpG island in KvLQT1 is associated with an antisense paternal transcript and loss of imprinting in Beckwith-Wiedemann syndrome. *Proc. Natl. Acad. Sci. USA*. 96:8064–8069. http://dx.doi.org/10.1073/pnas.96.14.8064

Spitale, R.C., M.C. Tsai, and H.Y. Chang. 2011. RNA templating the epigenome: long noncoding RNAs as molecular scaffolds. *Epigenetics*. 6:539–543. http://dx.doi.org/10.4161/epi.6.5.15221

Terranova, R., S. Yokobayashi, M.B. Stadler, A.P. Otte, M. van Lohuizen, S.H. Orkin, and A.H. Peters. 2008. Polycomb group proteins Ezh2 and Rnf2 direct genomic contraction and imprinted repression in early mouse embryos. *Dev. Cell*. 15:668–679. http://dx.doi.org/10.1016/j.devcel.2008.08.015

Thakur, N., V.K. Tiwari, H. Thomassin, R.R. Pandey, M. Kanduri, A. Göndör, T. Grange, R. Ohlsson, and C. Kanduri. 2004. An antisense RNA regulates the bidirectional silencing property of the Kcnq1 imprinting control region. *Mol. Cell. Biol.* 24:7855–7862. http://dx.doi.org/10.1128/MCB.24.18.7855-7862.2004

Thorvaldsen, J.L., K.L. Duran, and M.S. Bartolomei. 1998. Deletion of the H19 differentially methylated domain results in loss of imprinted expression of H19 and Igf2. *Genes Dev.* 12:3693–3702. http://dx.doi.org/10.1101/gad.12.23.3693

Wutz, A., O.W. Smrzka, N. Schweifer, K. Schellander, E.F. Wagner, and D.P. Barlow. 1997. Imprinted expression of the Igf2r gene depends on an intronic CpG island. *Nature*. 389:745–749. http://dx.doi.org/10.1038/39631

Yao, X., J.F. Hu, M. Daniels, H. Shiran, X. Zhou, H. Yan, H. Lu, Z. Zeng, Q. Wang, T. Li, and A.R. Hoffman. 2003. A methylated oligonucleotide inhibits IGF2 expression and enhances survival in a model of hepatocellular carcinoma. *J. Clin. Invest.* 111:265–273.

Zhang, H., B. Niu, J.F. Hu, S. Ge, H. Wang, T. Li, J. Ling, B.N. Steelman, G. Qian, and A.R. Hoffman. 2011. Interruption of intrachromosomal looping by CCCTC binding factor decoy proteins abrogates genomic imprinting of human insulin-like growth factor II. *J. Cell Biol.* 193:475–487. http://dx.doi.org/10.1083/jcb.201101021